

# Evaluation of Corneal Damage After Lacrimal Gland Excision in Male and Female Mice

Neal E. Mecum,<sup>1,2</sup> Dan Cyr,<sup>3</sup> Jennifer Malon,<sup>1</sup> Danielle Demers,<sup>1</sup> Ling Cao,<sup>1,3</sup> and Ian D. Meng<sup>1,3</sup>

<sup>1</sup>Center for Excellence in the Neurosciences, University of New England, Biddeford, Maine, United States

<sup>2</sup>Molecular and Biomedical Sciences, University of Maine, Orono, Maine, United States

<sup>3</sup>Department of Biomedical Sciences, College of Osteopathic Medicine, University of New England, Biddeford, Maine, United States

Correspondence: Ian D. Meng, Department of Biomedical Sciences, University of New England, 11 Hills Beach Road, Biddeford, ME 04106, USA; imeng@une.edu.

Submitted: December 16, 2018

Accepted: June 27, 2019

Citation: Mecum NE, Cyr D, Malon J, Demers D, Cao L, Meng ID. Evaluation of corneal damage after lacrimal gland excision in male and female mice.

*Invest Ophthalmol Vis Sci.*

2019;60:3264–3274. <https://doi.org/10.1167/iovs.18-26457>

**PURPOSE.** Lacrimal gland excision (LGE) has been utilized in several studies to model aqueous tear deficiency, yet sex as a biological variable has not been factored in to these reports. This study compared corneal pathology in male and female mice following LGE-induced dry eye.

**METHODS.** An LGE of either the extraorbital lacrimal gland (single LGE) or both the extraorbital and intraorbital lacrimal glands (double LGE) was performed in male and female C57BL/6J and Balb/cJ mice to produce dry eye of graded severity. Following excision, tearing was evaluated with phenol red thread, and corneal fluorescein staining was scored to quantify the severity of damage. Corneas were evaluated for apoptosis by the TUNEL assay and for cell proliferation using Ki67 staining. Furthermore, corneas were harvested and analyzed for macrophages via flow cytometry.

**RESULTS.** Baseline tearing levels were similar in male and female mice, and LGE resulted in comparable reductions in tearing with the lowest levels recorded after double LGE. As determined by fluorescein staining, LGE produced more severe damage to the cornea in female C57BL/6J and Balb/cJ mice. Double LGE increased TUNEL and Ki67 staining in the cornea, with greater increases found in female mice. Furthermore, LGE produced a greater increase in the total number of corneal macrophages in female mice.

**CONCLUSIONS.** These results indicate that female mice are more susceptible to LGE-induced corneal damage. The mechanisms involved in producing these sex differences still need to be elucidated but may involve increased inflammation and macrophage infiltration.

**Keywords:** dry eye, sex, lacrimal gland, apoptosis

Dry eye disease (DED) is a multifarious disease characterized by the sensation of ocular dryness and irritation that is commonly accompanied by tear deficiency.<sup>1</sup> The cause of DED can be related to attenuated tear quantity and/or altered tear composition, resulting in clinical presentations of tear film instability, inflammation and damage to the ocular surface, and ocular discomfort and pain.<sup>2</sup> Insufficient tear production by the lacrimal glands results in aqueous dry eye caused by a deficiency in the aqueous tear layer, whereas meibomian gland dysfunction results in evaporative dry eye due to the lack of a protective barrier created by the outer meibum lipid tear layer.<sup>2,3</sup> Population-based epidemiologic studies show a wide range of disease prevalence, from 5% to almost 35%, depending on the study population and operational definition of DED.<sup>4,5</sup> The incidence of DED increases with age, and dry eye symptoms are more frequently reported in women compared to men.<sup>6–9</sup>

Sex differences in animal models of dry eye have been previously reported. In particular, genetic mouse models of Sjögren's disease have shown significant differences in the inflammation of lacrimal and meibomian glands. For example, lacrimal glands in MRL-lpr mice show greater signs of inflammation in females compared to males, whereas the reverse is true in nonobese diabetic (NOD) mice, in which the lacrimal glands from male animals show greater signs of

inflammation.<sup>10,11</sup> Dry eye produced by desiccating environmental stress, usually presented with an anticholinergic drug, typically has been employed using only female animals.<sup>12–18</sup> However, one study that used female and male animals in the desiccating environmental stress model found a greater reduction in tears and increased corneal damage in female mice.<sup>19</sup>

In two additional models of aqueous tear deficiency, lacrimal gland excision (LGE) and injection of botulinum toxin B into the lacrimal gland, only female mice have been tested.<sup>16–18,20–22</sup> In contrast, LGE in the rat has been performed exclusively in male animals.<sup>23–30</sup> A direct comparison of female and male animals after LGE has not been performed.

Typical endpoints in animal models of dry eye include signs and symptoms of disease progression, such as tear quantity measured with a modified Schirmer's test and corneal epithelial cell damage as observed with corneal fluorescein staining.<sup>12,23,24,31–35</sup> Additional consequences of dry eye include corneal epithelial cell apoptosis, increases in the presence of distinct inflammatory markers, infiltration of immune cells to the ocular surface, and epithelial cell proliferation for their involvement in corneal wound healing.<sup>15–18,20,34–46</sup> It is currently unknown how sex might affect these common endpoints following LGE. The present study used LGE to compare the effect of aqueous tear deficiency in two strains of



male and female mice. A graded severity of dry eye was produced by excising either the extraorbital lacrimal gland (single LGE) or both the extraorbital and intraorbital lacrimal glands (double LGE).

## METHODS

### Animals

Male and female C57BL/6J and BALB/cJ mice aged 8 to 10 weeks were obtained from Jackson Labs (Bar Harbor, ME, USA) and housed in a controlled 12-hour light/dark cycle with free access to food and water. Animals were treated according to the policies and recommendations of the National Institutes of Health guidelines for the handling and use of laboratory animals and in accordance with the ARVO Statement for the Use of Animals in Ophthalmic and Vision Research. All procedures were approved by the Institutional Animal Care and Use Committee at the University of New England.

### Surgical Procedure

Unilateral LGE was performed under 1.5% to 2% isoflurane anesthesia. The extraorbital lacrimal gland was accessed through a 3-mm incision made anterior and ventral to the ear (Fig. 1A). The intraorbital lacrimal gland, located rostral to the extraorbital gland within the ventral orbit, was approached with a smaller 1-mm incision, taking care to avoid surrounding blood vessels and nerves (Fig. 1B). For the single LGE treatment group, only the larger extraorbital lacrimal gland was excised, whereas both the extraorbital and intraorbital lacrimal glands were excised in the double LGE treatment group. For sham surgeries, two incisions were made and both glands were partially exposed.

### Hematoxylin and Eosin Stain

To confirm gland tissue excision, extraorbital and intraorbital glands were fixed in formalin following removal and embedded in paraffin, and 5- $\mu$ m sections were cut on a microtome. Slides were dried overnight at ambient temperature and baked at 60°C for 1 hour. Slides were dewaxed, rehydrated, and stained with hematoxylin and eosin on a Leica Autostainer XL (Leica, Buffalo Grove, IL, USA), then dehydrated through graded alcohols, cleared with xylene, and mounted using a resinous mounting medium.

### Tear Measurements

Tears were measured by inserting cotton phenol red threads (Zone-Quick; FCI Ophthalmic, Pembroke MA, USA) into the lateral canthus of the eye for 20 seconds in unanesthetized animals. The length of thread presenting with a change in color was measured under a microscope to the nearest 0.1 mm.

### Fluorescein

Corneal fluorescein staining was performed every week beginning the first week before surgery in order to assess the degree of corneal damage after LGE. A 1% fluorescein solution (10  $\mu$ L; Sigma-Aldrich Corp., St. Louis, MO, USA) was applied to the cornea in isoflurane-anesthetized animals. After 2 minutes, the eye was rinsed with artificial tears to remove excess fluorescein and examined using cobalt blue light from an ophthalmic slit-lamp handheld model scope (Hai Laboratories, Inc., Lexington, MA, USA). The degree of staining was scored based on a 0 to 4 grading system.<sup>23,33</sup> The absence of fluorescein staining was scored with a 0; staining of up to 1/

8 of the cornea was scored a 1; between 1/8 and 1/4 of the cornea was scored a 2; 1/4 to 1/2 of the cornea was scored a 3; and greater than 1/2 of the cornea was scored a 4.

### TUNEL and Ki67 Staining

Cell death due to apoptosis was identified via TUNEL assay using an in situ cell death detection kit (TMR Red; Roche, Nutley, NJ, USA). Corneas were harvested and fixed in 10% formalin overnight, and then in 30% sucrose for 3 days. Frozen corneal cross sections were cut at 12  $\mu$ m using a cryostat, and mounted sections were stored at -80°C. For TUNEL staining, corneas were briefly washed in phosphate-buffered saline (PBS), permeabilized with PBS-Triton (T) for 15 minutes, and stained in accordance with the manufacturer's directions. Following TUNEL staining, corneas were processed for Ki67 protein (ab16667; Abcam, Cambridge, MA, USA), a cellular proliferation marker expressed only during active stages of the cell cycle. Corneal tissue was briefly washed in PBS, permeabilized with PBS-T for 15 minutes, and blocked with 5% normal donkey serum in PBS-T for 1 hour. Following blocking solution, 1:100 diluted primary Ki67 antibody was applied and incubated overnight. After brief washes in PBS, tissue was incubated with a FITC anti-rabbit secondary antibody (1:200; Thermo Fisher Scientific, Portsmouth, NH, USA) for 1 hour. Slides were then coverslipped with a Vectashield soft-set medium with 4',6-diamidino-2-phenylindole (DAPI) (Vector Labs, Burlingame, CA, USA).

Actively proliferating and apoptotic cells were identified using a fluorescence microscope (Leica DM2500M) with LAS V4.6 software. For each cornea, four sagittal sections that crossed through the corneal apex were selected for analysis. In each section, two regions were defined based on their distance from the corneal apex. The central zone consisted of an area within 0.75 mm of the corneal apex, and the peripheral zone was located just outside of the measured corneal center. Harvested corneas did not include the limbus or conjunctiva. Two images were taken from each region by a researcher blinded to the animal's treatment and sex. From these images, TUNEL-positive (TUNEL+) and Ki67-positive (Ki67+) staining was counted by two blinded researchers. Overall counts from the two researchers differed by <5% and were averaged for the final analysis. Comparisons were made between treatment groups after calculating the mean of the counts from all eight regions.

### Flow Cytometry

Frequencies of macrophages and dendritic cells present in the cornea were examined using flow cytometry. Corneas, not including limbal or conjunctival areas, were harvested and six corneas from each treatment group were pooled into 2-mL conical tubes. Tissue was digested with 2 mg/mL collagenase (11088858001, Sigma-Aldrich Corp.) and 0.5 mg/mL DNase (04716728001, Sigma-Aldrich Corp.) in Hanks' balanced salt solution (Lonza Biologics, Portsmouth, NH, USA). The corneas were agitated on a tube shaker at 400 rpm at 37°C for 2.5 to 3 hours. Each sample was titrated with a Pasteur pipette and filtered with a 70- $\mu$ m mesh filter. The filters were flushed with 3.5 mL 20 mM EDTA (pH 7.4). After samples were washed with PBS, they were stained with 5(6)-carboxyfluorescein diacetate N-succinimidyl ester (CFSE, Sigma-Aldrich Corp.) per the manufacturer's instructions. Pellets were washed with PBS for 5 minutes and then cell surface Fc receptors were blocked by anti-mouse CD16/CD32 (clone 2.4G2, 50  $\mu$ L at 1  $\mu$ g/mL, 553142; BD Biosciences, San Diego, CA, USA) for 30 minutes on ice. CD45 and CD11b fluorescent-labeled monoclonal antibodies were used to identify infiltrating cells (APC anti-

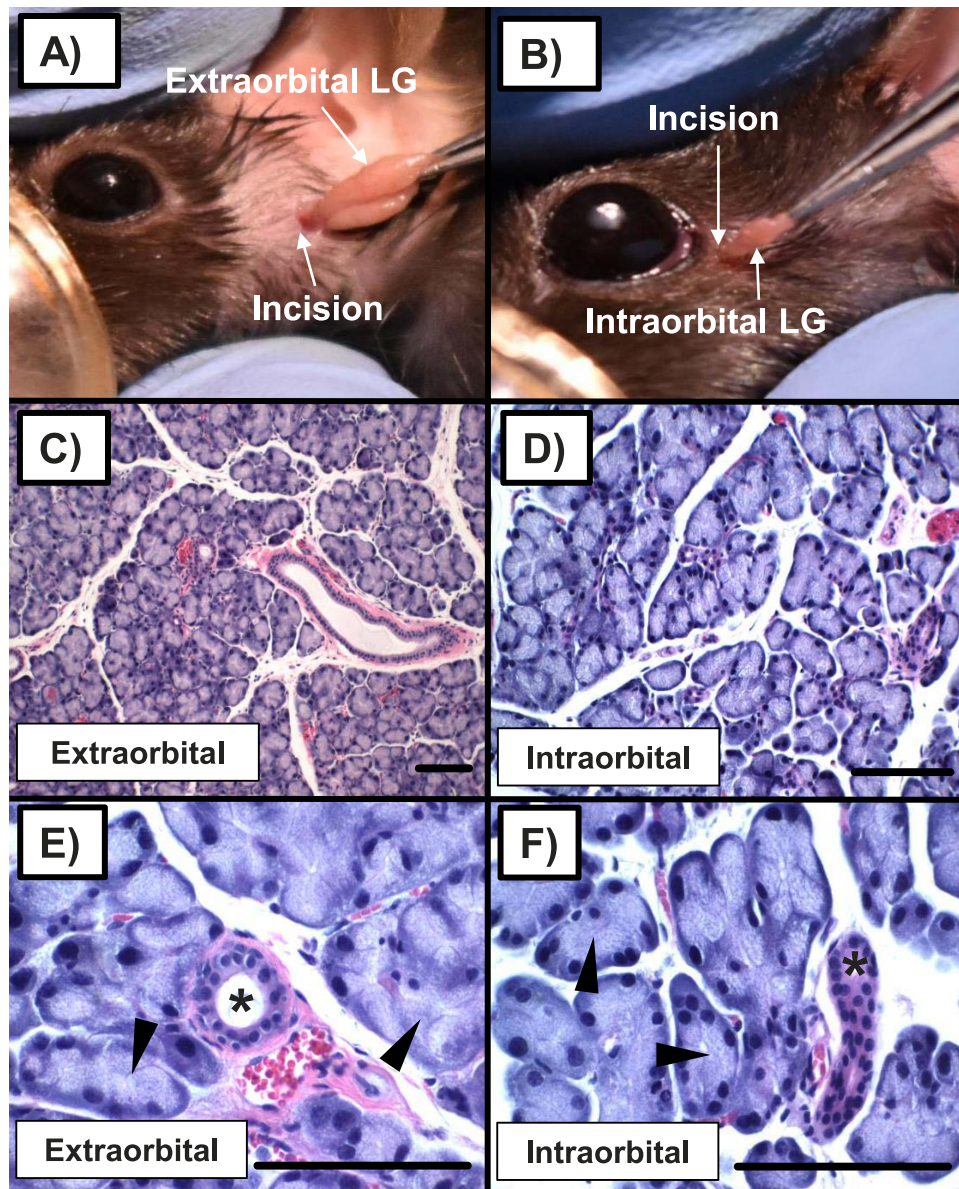


**FIGURE 1.** Extraorbital and intraorbital lacrimal gland histology from hematoxylin- and eosin-stained tissue. (A, B) Photographs showing the incisions performed for excision of the (A) extraorbital lacrimal gland and (B) smaller intraorbital lacrimal gland. (C) Photomicrograph of an extraorbital lacrimal gland section illustrating acinar cells surrounded by myoepithelial cells, blood vessels, and ductal epithelial cells. (D) Intraorbital lacrimal gland section showing similar characteristics to the extraorbital lacrimal gland. (E) Increased magnification of the extraorbital gland demonstrates acinar cells (*arrows*) and an intra- or interlobular excretory duct (*asterisk*). (F) An intraorbital lacrimal gland section with similar acinar cells (*arrows*) and excretory ducts (*asterisk*). LG, lacrimal gland. Scale bars: 100  $\mu\text{m}$ .

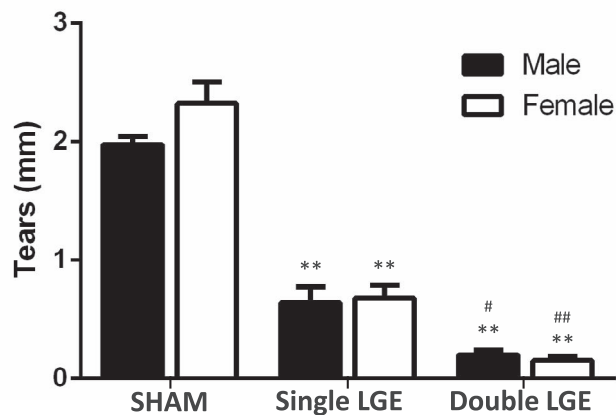
mouse CD45 clone 30-11, and PE anti-mouse CD11b clone M1/70, both at 1:50; Thermo Fisher). After incubation for 30 minutes on ice, 500  $\mu\text{L}$  PBS was added and centrifuged at 2000g 4°C for 5 minutes. Supernatant was removed and samples were washed again with PBS. The samples were run on a C6 Accuri Flow Cytometer (BD Biosciences) along with nonstained controls at each time. Data were analyzed using FlowJo software (Tree Star, Inc., Ashland, OR, USA).

### Statistical Analysis

Multiple comparisons for parametric data sets with normal distributions and equal variance were analyzed using a 2-way

ANOVA without repeated measures and a Tukey post hoc test. Data sets analyzed in this way (with sex and surgery as the two factors) included tear measurements, Ki67+ and TUNEL+ cell values, and flow cytometric data. Fluorescein scores across the 4-week time period were analyzed using Friedman repeated measures analysis of variance on ranks with Dunn's post hoc analysis. Fluorescein sex differences for individual time points and treatments were determined using a Mann-Whitney *U* test. Analyses were performed using commercial software (GraphPad Prism 6; GraphPad Software, San Diego, CA, USA). All results are expressed as mean  $\pm$  SEM. Values of  $P < 0.05$  were considered to be statistically significant.

## A) C57BL/6J



## B) BALB/cJ

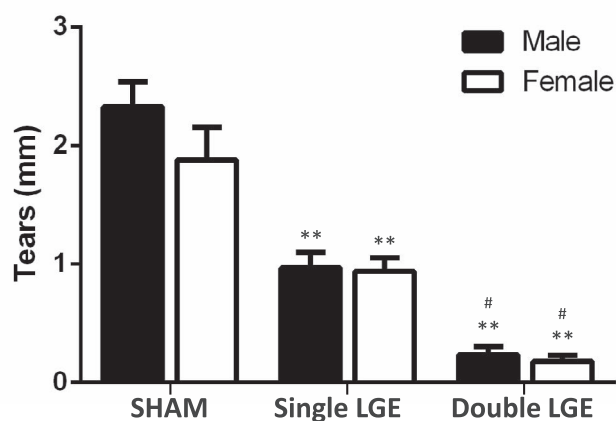


**FIGURE 2.** The effect of lacrimal gland excision (LGE) on tear levels in (A) C57BL/6J mice and (B) BALB/cJ mice. Tears were quantified using a cotton phenol red thread 2 weeks post surgery. In both mouse strains, excision of the extraorbital lacrimal gland (single LGE) reduced tears when compared with sham surgery, with excision of both the extraorbital and intraorbital lacrimal glands (double LGE) producing a further reduction in tears. No differences were observed between male and female mice. \*\* $P < 0.01$  versus sham; # $P < 0.05$  and ## $P < 0.01$  versus single LGE;  $n = 12$  to  $24$  for C57BL/6J mice;  $n = 17$  or  $18$  for BALB/cJ mice.

## RESULTS

## Extraorbital and Intraorbital Lacrimal Gland Histology

To verify the accuracy of intraorbital and extraorbital LGEs, lacrimal gland tissue from C57BL/6J mice was examined following hematoxylin and eosin staining (Fig. 1). The extraorbital gland, located just anterior to the ear, was easily identified prior to excision (Fig. 1A). The gross morphology of the much smaller intraorbital gland was similar to that of the extraorbital gland, yet its location was entirely within the inferior orbit (Fig. 1B). The extraorbital gland demonstrated a multilobed, tubule-alveolar exocrine gland structure (Fig. 1C), consisting of mostly acinar cells surrounded by myoepithelial cells, blood vessels, and intra- and interlobular ducts (Fig. 1E). The general features of the intraorbital gland were similar to those of the extraorbital gland (Figs. 1D, 1F).

## Quantification of Tears

Cotton phenol red threads were used to assess the extent of aqueous tear loss 2 weeks following sham, single, and double LGE in male and female mice. In male and female C57BL/6J mice, single LGE reduced tear levels by 67% to 70% relative to sham-treated animals, while double LGE produced an 89% to 93% reduction compared to sham treatment. A significant surgical effect was found using a 2-way ANOVA to compare group mean averages in C57BL/6J mice (Fig. 2A; Table). A Tukey post hoc analysis revealed a reduction in tears measured from both male and female mice following single and double LGE compared to sham controls ( $P < 0.001$ ), with double LGE producing an even greater reduction when compared to single LGE (male mice,  $P < 0.05$ ; female mice,  $P < 0.01$ ). Likewise, for BALB/cJ mice (Fig. 2B), a 2-way ANOVA to compare group mean averages also showed a significant surgical treatment effect (Table). After single LGE, male and female mice had 49% to 58% lower tear levels compared to sham animals ( $P < 0.01$ ). Double LGE produced an even greater 89% to 90% reduction in tears compared to sham ( $P < 0.01$ ), which was also significantly lower than after single LGE ( $P < 0.05$ ). No sex-specific differences were found in tear levels following LGE for either C57BL/6J or BALB/cJ mice (Table).

## Fluorescein Scores in C57BL/6J and BALB/cJ Mice

To assess corneal damage following LGE, fluorescein was visualized each week after surgery using a slit-lamp ophthalmoscope. Sham surgery did not alter corneal fluorescein staining in male or female mice across the 4-week observation period in either the C57BL/6J or BALB/cJ mice (Figs. 3A, 3B). Following single LGE in C57BL/6J mice, female mice had significantly higher fluorescein scores at 2 and 3 weeks post surgery compared to male mice at the same time points (Fig. 3C,  $P < 0.01$  for week 2 and  $P < 0.05$  for week 3). This difference was primarily due to a reduction in male fluorescein scores after the first week. Double LGE produced an even greater elevation in fluorescein scores, with male and female C57BL/6J mice showing peak scores at 1 week post surgery (Fig. 3E). At weeks 2 and 3, however, male mice demonstrated an ability to recover significantly, as indicated by lower fluorescein scores compared to week 1 (Fig. 3E,  $P < 0.01$ ). In contrast, fluorescein scores in female mice remained elevated throughout the 4 weeks.

When compared to C57BL/6J mice, LGE in BALB/cJ mice produced far less severe corneal epithelial cell damage. Consistent with C57BL/6J mice, however, was the finding that female BALB/cJ mice demonstrated a more severe corneal pathology after LGE. After single LGE in BALB/cJ mice, the only significant increase in fluorescein scores was at the 2-week time point, with female mice exhibiting higher fluorescein scores compared to their male counterparts (Fig. 3D,  $P < 0.05$ ). Following double LGE in BALB/cJ mice, both female and male animals had increased fluorescein scores above baseline values, yet female mice had greater fluorescein scores at every time point compared to male mice (Fig. 3E,  $P < 0.01$ ). Unlike the C57BL/6J mice, male mice did not exhibit a greater elevation in fluorescein scores at week 1, instead showing a consistently lower level throughout the 4-week observation period.

## Apoptosis of Corneal Epithelial Cells

Quantification of TUNEL+ cells was performed to assess corneal epithelial cell apoptosis following LGE in C57BL/6J mice (Fig. 4). The TUNEL stain, a method for identifying cells undergoing DNA degradation due to apoptosis, produced an

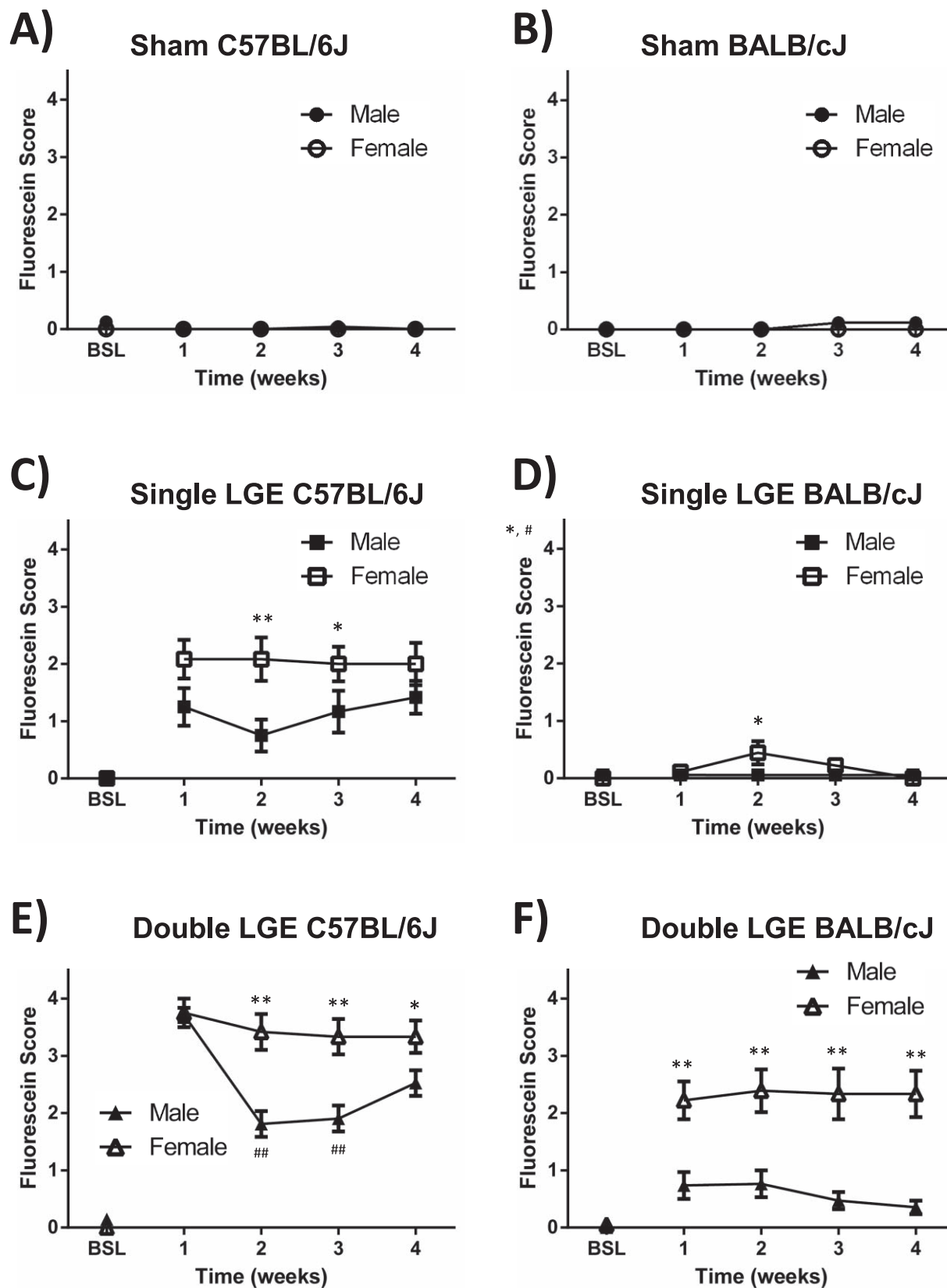


**FIGURE 3.** Corneal fluorescein scores following lacrimal gland excision. The cornea was examined prior to and each week following surgery. Both single and double LGE produced greater corneal damage in C57BL/6J compared to BALB/cJ mice. In both strains, however, female mice showed greater corneal damage compared to male mice. (A, B) Corneal fluorescein scores following sham surgery in C57BL/6J and BALB/cJ mice. (C, D) Corneal fluorescein scores following single LGE surgery in C57BL/6J and BALB/cJ mice. (E, F) Corneal fluorescein scores following double LGE surgery in C57BL/6J and BALB/cJ mice. \* $P < 0.01$  and \*\* $P < 0.01$  for female versus male mice at the same time point; ## $P < 0.01$  versus male animals at 1 week;  $n = 12$  to 24 per treatment group.

TABLE. Results From ANOVA Statistical Analysis for All Data Sets

Figure	Measurement (Units)	Sex			Surgery			Interaction		
		dfn, dfd	F	P	dfn, dfd	F	P	dfn, dfd	F	P
Figure 2A	Tears (mm)	1, 90	2.077	<0.153	2, 90	253.9	<0.0001	2, 90	2.578	<0.0815
Figure 2B	Tears (mm)	1, 99	1.78	<0.1852	2, 99	69.51	<0.0001	2, 99	1.038	<0.3581
Figure 4A	Wk 1 (No. of Ki67 cells)	1, 30	3.756	<0.0621	2, 30	54	<0.0001	2, 30	5.16	<0.0119
Figure 4A	Wk 2 (No. of Ki67 cells)	1, 30	2.251	<0.1440	2, 30	38.79	<0.0001	2, 30	1.001	<0.3795
Figure 4A	Wk 4 (No. of Ki67 cells)	1, 30	1.23	<0.2763	2, 30	21.37	<0.0001	2, 30	0.035	<0.9671
Figure 5A	Wk 1 (No. of TUNEL cells)	1, 30	7.95	<0.0084	2, 30	37.42	<0.0001	2, 30	3.756	<0.0350
Figure 5A	Wk 2 (No. of TUNEL cells)	1, 30	1.623	<0.2125	2, 30	16.34	<0.0001	2, 30	1.738	<0.1932
Figure 5A	Wk 4 (No. of TUNEL cells)	1, 30	10.49	<0.0029	2, 30	11.76	<0.0002	2, 30	7.977	<0.0017
Figure 6C	Wk 1 (% CD45 <sup>+</sup> cells)	1, 15	2.993	<0.1041	2, 15	4.893	<0.0231	2, 15	2.884	<0.0871
Figure 6C	Wk 2 (% CD45 <sup>+</sup> cells)	1, 12	0.69	<0.4223	2, 12	3.912	<0.0492	2, 12	1.412	<0.2813
Figure 6D	Wk 1 (% CD11b <sup>+</sup> /CD45 <sup>+</sup> )	1, 15	1.752	<0.2055	2, 15	13.12	<0.0005	2, 15	6.078	<0.0117
Figure 6D	Wk 2 (% CD11b <sup>+</sup> /CD45 <sup>+</sup> )	1, 12	2.346	<0.1515	2, 12	18.74	<0.0002	2, 12	3.954	<0.0480

Sex and surgery were the two factors (independent variables) used in the 2-way ANOVAs. dfn, degrees of freedom numerator; dfd, degrees of freedom denominator; F, F statistic.

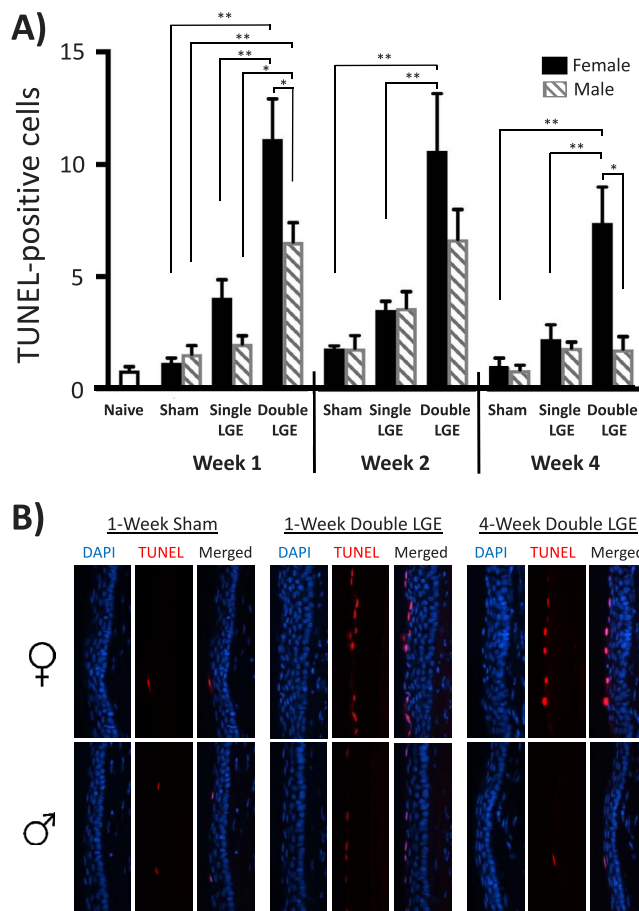


FIGURE 4. Apoptosis of corneal epithelial cells following lacrimal gland excision. (A) Quantification of TUNEL in corneal cross sections 1, 2, and 4 weeks post surgery. At 1 and 4 weeks, double LGE in female mice produced a greater number of TUNEL-positive cells compared to male mice. (B) Representative images for TUNEL-positive cells at 1, 2, and 4 weeks post surgery. Note the increase in TUNEL-positive cells in female mice (upper), which were mainly located in the superficial epithelium, compared to the male mice (lower). Cell nuclei were stained with DAPI. \* $P < 0.05$ , \*\* $P < 0.01$ ;  $n = 6$  per treatment group.

easily identifiable punctate label located in the outer epithelial cell layers of the cornea (Fig. 4B). Each time point was analyzed using a 2-way ANOVA for group mean averages with Tukey post hoc analysis for surgical and/or sex differences (Fig. 4A). At weeks 1, 2, and 4, there was a significant effect of surgery on the number of TUNEL+ cells (Table).

A significant effect of sex was found only at weeks 1 and 4 (Table). Post hoc analysis revealed a greater number of TUNEL+ cells in female and male animals after double LGE at week 1 when compared to both sham surgery ( $P < 0.01$ ) and single LGE (female mice,  $P < 0.01$ ; male mice,  $P < 0.05$ ). At weeks 2 and 4, TUNEL+ cells were elevated only in female animals after double LGE compared to sham and single LGE treatment ( $P < 0.01$ ). The increase in TUNEL+ cells after single LGE did not reach significance at any of the time points. At 1 and 4 weeks post surgery, double LGE in female mice produced significantly more TUNEL+ cells than in male mice ( $P < 0.05$ ), while the sex difference at 2 weeks post surgery failed to reach significance. Sham surgery did not alter the number of TUNEL+ cells at any time point when compared to naïve animals (Fig. 4A).

### Corneal Epithelial Cell Proliferation

Corneal epithelial cell proliferation was examined using an antibody against Ki67 in C57BL/6J mice (Fig. 5). Ki67 is a protein expressed only during the active phases of the cell cycle<sup>47</sup> and can be seen expressed in corneal epithelial cells in both sham and LGE treatment groups (Fig. 5B). Each time point was analyzed using a 2-way ANOVA for group mean averages with a Tukey post hoc analysis for surgical and/or sex differences. A significant effect of surgery treatment was found at all three time points, whereas an effect of sex was observed only at the first week after surgery (Table). Post hoc analysis revealed an increase in the number of Ki67+ cells in both male and female animals after double LGE at all three time points (Fig. 5A,  $P < 0.01$  versus sham;  $P < 0.05$  versus single LGE). At 1 week, the number of Ki67+ cells was significantly greater in female animals compared to their male counterparts (Fig. 5A,  $P < 0.05$ ). After single LGE, the increase in Ki67+ cells did not reach statistical significance (Fig. 5A,  $P > 0.05$ ). As with TUNEL staining, sham surgery did not alter the number of Ki67+ cells when compared to naïve animals.

### Flow Cytometric Analysis of Infiltrating Cells

Frequencies of macrophages and dendritic cells were examined using flow cytometry (Fig. 6). Pooled corneas from six

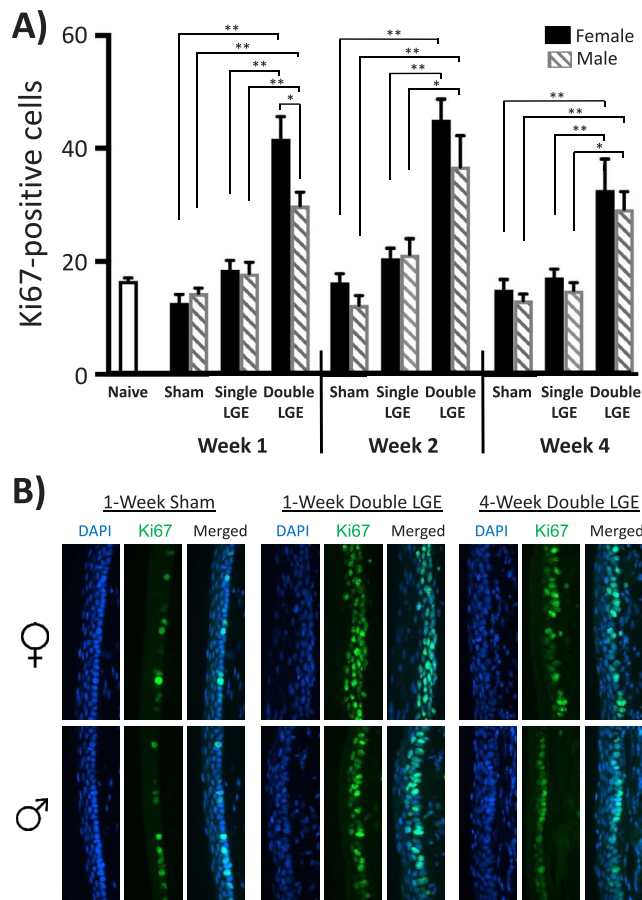


**FIGURE 5.** Corneal epithelial cell proliferation following lacrimal gland excision. (A) Quantification of Ki67 in corneal cross sections 1, 2, and 4 weeks post surgery. At 1 week, double LGE in female mice caused significantly more cell proliferation when compared to male mice. At the other time points, double LGE produced similar increases in Ki67-positive cells in female and male mice. (B) Representative images of Ki67-positive cells at 1, 2, and 4 weeks post LGE. Cell nuclei are stained with DAPI. \* $P < 0.05$ , \*\* $P < 0.01$ ;  $n = 6$  per treatment group.

mice were used for each sample and data were analyzed from three independent experiments. A comparison of group means between populations of CD45<sup>+</sup> cells in cornea samples found an overall difference between surgery treatment groups at the 1- and 2-week time points ( $P < 0.05$ , Table), with no significant effect of sex ( $P > 0.05$ , Table). Individual group comparisons did not reveal a significant difference between any two individual treatment groups ( $P > 0.05$ , Fig. 6C). An analysis of the percentage of CD45<sup>+</sup>/CD11b<sup>+</sup> cells (mostly macrophages, neutrophils, and dendritic cells) indicated a significant effect of both surgery ( $P < 0.01$ , Table) and sex ( $P < 0.01$ , Table) at the 1- and 2-week time points. One week after both single and double LGE, female mice showed a greater percentage of CD45<sup>+</sup>/CD11b<sup>+</sup> cells when compared to sham controls (Fig. 6D). In male mice, single but not double LGE increased the percentage of CD45<sup>+</sup>/CD11b<sup>+</sup> cells at 1 week (Fig. 6D). At 2 weeks post surgery, corneas from female mice with double LGE had a greater percentage of CD45<sup>+</sup>/CD11b<sup>+</sup> cells when compared to sham, single LGE, and male mice with double LGE (Fig. 6D). In contrast, the percentage of CD45<sup>+</sup>/CD11b<sup>+</sup> cells in male mice was not significantly elevated 2 weeks after single or double LGE when compared to sham controls (Fig. 6D).

## DISCUSSION

In this study, the effects of LGE-induced dry eye on corneal pathology in female and male mice were compared. While LGE produced a comparable reduction in tearing, female mice, both C57BL/6J and BALB/cJ strains, showed elevated corneal fluorescein scores when compared to male mice. Consistent with this observation of greater corneal damage, female mice also demonstrated greater increases in corneal epithelial cell apoptosis and immune cell infiltration. In both sexes, excision of only the extraorbital lacrimal gland (single LGE) caused milder corneal pathology when compared to excision of both the extraorbital and intraorbital lacrimal gland (double LGE). However, even the more moderate manifestation of dry eye after single LGE was more pronounced in female mice.

Previous studies in the mouse and rat have utilized LGE to study the effects of reduced aqueous tearing on the cornea. In these studies, most excised only the extraorbital lacrimal gland; however, one study in mouse and one in rat have compared the consequences of double LGE to single LGE.<sup>21,23</sup> Histologic comparison of the intraorbital and extraorbital lacrimal glands confirmed their morphologic similarities, with both glands demonstrating lobules lined with secreting acinar cells, as has been previously described.<sup>21</sup> As lacrimal glands are the primary source of the aqueous component of tears, including water, electrolytes, and proteins, a reduction in secretions from the lacrimal gland results in aqueous tear deficiency.<sup>31,48</sup> Consistent with the present study, single and double LGE have been shown to cause a graded reduction in tear volume, matched by an increase in corneal fluorescein staining.<sup>21,23</sup> The ability to create a reproducible dry eye with graded severity without the use of pharmaceuticals (e.g., anticholinergic drugs) represents a particular advantage of this model.<sup>20</sup>

The comparison of single and double LGE in the rat has been performed using exclusively male animals, whereas in the mouse, female C57B/6 animals were used.<sup>21,23</sup> Similarly, studies employing excision of only the extraorbital lacrimal gland have utilized either only male or female animals. In general, studies performed in rats have used males,<sup>23-30</sup> and studies in mice have used females.<sup>20-22</sup> The utilization of female C57B/6 mice by Stevenson et al.<sup>20</sup> likely contributed to their conclusion that single LGE results in severe dry eye symptoms, with extensive damage to the corneal epithelium. In contrast, we found that single LGE in male animals produced a considerably less severe manifestation of dry eye. It also should be noted that these differences were found without controlling for the stage of estrous, and fluctuating levels of estrogen and progesterone during the estrous cycle could further impact corneal properties and immune responses to LGE.

In addition to sex, mouse strain also had a significant impact on the severity of dry eye observed after LGE. Baseline tearing and the amount of tear reduction following LGE was comparable for both strains, yet a much more severe phenotype was expressed in both male and female C57BL/6J mice. Strain differences have also been noted as a result of desiccating environmental stress.<sup>17,49</sup> Following exposure to a dry environment, a greater reduction in tear production was found in female C57BL/6 mice when compared to female BALB/c mice, yet similar increases in corneal fluorescein scores were noted.<sup>49</sup> Furthermore, while both C57BL/6 and BALB/c mice showed a decrease in conjunctival goblet cell density after 3 days of dry environment exposure, only the BALB/c mice demonstrated a capacity to recover after 7 days of exposure.<sup>49</sup> These results indicate that BALB/c mice may have a higher ability to compensate when presented with challenges to ocular homeostasis.

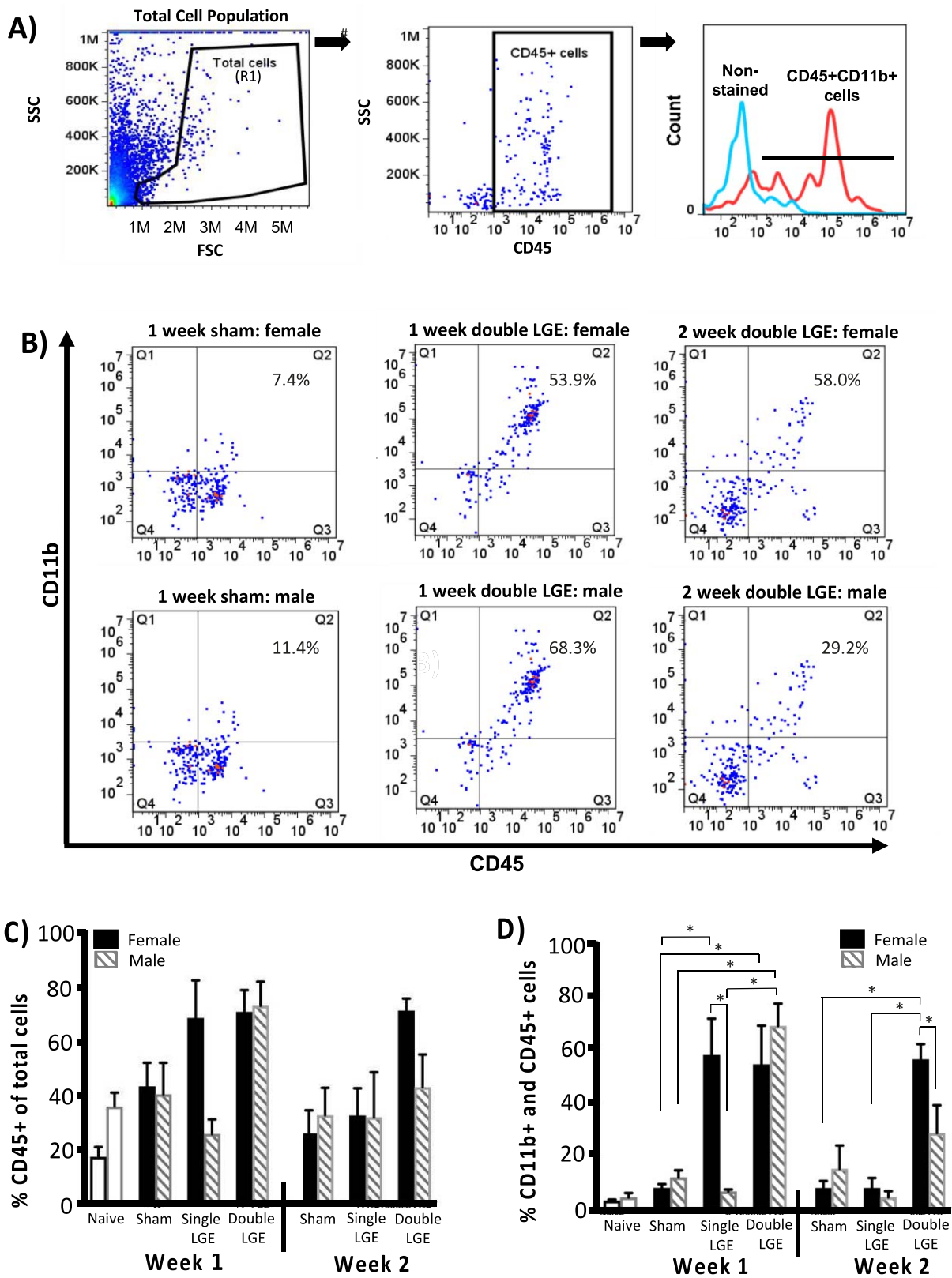


**FIGURE 6.** Antigen-presenting  $CD45^+/CD11b^+$  cells present in the cornea after lacrimal gland excision. **(A)** The total population of cells identified by the side scatter (SSC) versus forward scatter (FSC) dot plot, with cells falling within the region (R1) demarcated for further analysis.  $CD45^+$  cells were gated within the total cell population and cells positive for both  $CD45$  and  $CD11b$  were further identified and quantified. **(B)** Representative  $CD45$  versus  $CD11b$  dot plots for each of the six individual treatment groups, with the average percentages of  $CD45^+/CD11b^+$  cells within the total cell population labeled within each plot. **(C)** The percentage of  $CD45^+$  cells. **(D)** Percentage of  $CD45^+/CD11b^+$  cells. Data are from three separate runs with each sample consisting of six corneas.  $*P < 0.05$ .



Similar mouse strain differences have been found after corneal injury. After corneal epithelial debridement, the frequency of recurrent epithelial erosions was greater in C57BL/6 mice compared to BALB/c mice.<sup>50</sup> In addition, benzalkonium chloride-induced injury produced more severe corneal wounds in C57BL/6 mice.<sup>51</sup> These strain differences in the response to both dry eye and corneal injury have been attributed to differences in immune responses. In particular, C57BL/6 mice demonstrate a greater type 1 T helper cell (Th1) response, whereas BALB/c mice show a bias toward the type 2 T helper cell (Th2).<sup>52</sup> The Th1 response manifests as high interferon (IFN)- $\gamma$  secretion and low interleukin (IL)-4 secretion. In contrast, Th2-mediated immune responses are characterized by low IFN- $\gamma$  secretion and high IL-4. In C57BL/6 mice, desiccating stress-induced dry eye caused a greater increase in Th1 cell attracting chemokines on the ocular surface, including CCL3 and CCL4, when compared to BALB/c mice.<sup>17</sup> Since these are proinflammatory chemokines and also attract monocytes, macrophage infiltration may also play a role in the more severe dry eye observed in C57BL/6 mice after LGE.

Previous studies have examined corneal epithelial cell apoptosis in response to desiccating stress-induced dry eye.<sup>16,34</sup> As in the present study, an increase in apoptosis was observed concomitant to increases in fluorescein staining. We also found that levels of TUNEL staining were higher in female mice compared to males, which was consistent with the more extensive ocular surface damage observed with corneal fluorescein staining. Perhaps as a consequence of the increase in cell death, both male and female mice demonstrated an increase in cell proliferation after LGE, a result also seen after desiccating stress-induced dry eye in female mice.<sup>14</sup> This increase in epithelial cell turnover would likely assist in corneal wound healing. While TUNEL staining in male mice returned to baseline levels by 4 weeks post double LGE the number of Ki67+ cells remained elevated, indicating that cell proliferation may contribute to the decrease over time in fluorescein scores in male mice.

Tear deficiency results in ocular inflammation, contributing to dry eye symptoms.<sup>15,17,18,20,39-44</sup> In addition to increased production of proinflammatory cytokines and chemokines, dry eye results in the infiltration of immune cells including T cells, macrophages, dendritic cells, and neutrophils. Furthermore, inhibition of this inflammatory response can improve the clinical signs of dry eye.<sup>34,42</sup> Previous studies in female mice have shown significant infiltration of CD11b<sup>+</sup> cells, macrophages, and a subset of dendritic cells following desiccating stress-induced dry eye.<sup>34,45</sup> Consistent with these findings, both single and double LGE in female mice increased the percentage of CD45<sup>+</sup>/CD11b<sup>+</sup> cells, with double LGE elevating levels at both 1 and 2 weeks post LGE. In contrast, the percentage of CD45<sup>+</sup>/CD11b<sup>+</sup> cells in male mice increased only in the first week following double LGE. These sex differences in the immune response to LGE may contribute to the more severe corneal damage observed in female animals.

Sex differences in the extent of corneal damage and the immune response to ocular dryness have also been reported after desiccating stress-induced aqueous tear deficiency.<sup>19</sup> Exposure to a low-humidity environment caused a greater increase in corneal fluorescein staining in female mice at days 3 and 5, although comparable fluorescein scores were obtained in female and male mice at day 10. Corneal damage correlated with greater T-cell activation in female mice compared to males. In another corneal injury model, female mice took longer than male mice to heal following repeated cornea epithelial abrasions.<sup>53</sup> This delay in wound healing could be induced in male mice by topical corneal application of estrogen, indicating the importance of sex steroids in regulating wound healing. The delayed corneal wound healing

in female mice is consistent with a reported increase in re-epithelialization time in females compared to males when treated for fungal corneal ulcers.<sup>54</sup> Sex differences in gene expression from human corneas offer additional support for greater healing capacity in males.<sup>55</sup> For example, corneas from males demonstrated higher expression levels of epidermal growth factor receptor and genes that promote DNA replication and corneal epithelial cell migration.

The impact of sex on inflammation in DED is also supported by results from mouse models of Sjögren's syndrome.<sup>10,11</sup> Increased expression of proinflammatory genes in the lacrimal gland has been reported in female MRL-lpr mice and male NOD mice, consistent with the pathophysiology found in these mouse models. In the case of MRL-lpr mice, testosterone appears to play an important role in the suppression of the immune response and increased functioning of the lacrimal gland in male mice.<sup>56,57</sup> While the present study focused on the influence of sex in a model of aqueous tear deficiency, sex also likely impacts evaporative dry eye. Loss of meibomian gland function observed after the knockout of the epithelial sodium channel, beta-ENaC, from the meibomian gland resulted in greater corneal damage in female compared to male mice.<sup>58</sup> In this case, androgens may have played a protective role, as testosterone has been demonstrated to regulate genes involved in lipogenesis in meibomian gland tissue.<sup>59,60</sup>

In summary, female mice showed greater susceptibility of the cornea to damage after both single and double LGE that was time-dependent. Importantly, the strain of mouse also influenced the extent of corneal damage following LGE. Results from this study indicate that sex differences in inflammation of the ocular surface may contribute to the increase in dry eye-induced epithelial cell damage in female mice. Further studies are needed to determine the potential contribution of estrogen and testosterone to dry eye-induced inflammation in the LGE model.

### Acknowledgments

Supported by National Institutes of Health Grants P20GM103643 and R01EY026145 (IDM).

Disclosure: N.E. Mecum, None; D. Cyr, None; J. Malon, None; D. Demers, None; L. Cao, None; I.D. Meng, None

### References

1. Belmonte C, Nichols JJ, Cox SM, et al. TFOS DEWS II pain and sensation report. *Ocul Surf*. 2017;15:404-437.
2. Bron AJ, de Paiva CS, Chauhan SK, et al. TFOS DEWS II pathophysiology report. *Ocul Surf*. 2017;15:438-510.
3. Chhadva P, Goldhardt R, Galor A. Meibomian gland disease: the role of gland dysfunction in dry eye disease. *Ophthalmology*. 2017;124:S20-S26.
4. The epidemiology of dry eye disease: report of the Epidemiology Subcommittee of the International Dry Eye WorkShop (2007). *Ocul Surf*. 2007;5:93-107.
5. Stapleton F, Alves M, Bunya VY, et al. TFOS DEWS II epidemiology report. *Ocul Surf*. 2017;15:334-365.
6. Moss SE, Klein R, Klein BE. Prevalence of and risk factors for dry eye syndrome. *Arch Ophthalmol*. 2000;118:1264-1268.
7. Schaumberg DA, Dana R, Buring JE, Sullivan DA. Prevalence of dry eye disease among US men: estimates from the Physicians' Health Studies. *Arch Ophthalmol*. 2009;127:763-768.
8. Schaumberg DA, Sullivan DA, Buring JE, Dana MR. Prevalence of dry eye syndrome among US women. *Am J Ophthalmol*. 2003;136:318-326.

9. Sullivan DA, Rocha EM, Aragona P, et al. TFOS DEWS II Sex, gender, and hormones report. *Ocul Surf*. 2017;15:284-333.
10. Tellefsen S, Morthen MK, Richards SM, et al. Sex effects on gene expression in lacrimal glands of mouse models of Sjogren syndrome. *Invest Ophthalmol Vis Sci*. 2018;59:5599-5614.
11. Toda I, Sullivan BD, Rocha EM, Da Silveira LA, Wickham LA, Sullivan DA. Impact of gender on exocrine gland inflammation in mouse models of Sjogren's syndrome. *Exp Eye Res*. 1999;69:355-366.
12. Dursun D, Wang M, Monroy D, et al. A mouse model of keratoconjunctivitis sicca. *Invest Ophthalmol Vis Sci*. 2002;43:632-638.
13. Barabino S, Shen L, Chen L, Rashid S, Rolando M, Dana MR. The controlled-environment chamber: a new mouse model of dry eye. *Invest Ophthalmol Vis Sci*. 2005;46:2766-2771.
14. Fabiani C, Barabino S, Rashid S, Dana MR. Corneal epithelial proliferation and thickness in a mouse model of dry eye. *Exp Eye Res*. 2009;89:166-171.
15. Shen L, Barabino S, Taylor AW, Dana MR. Effect of the ocular microenvironment in regulating corneal dendritic cell maturation. *Arch Ophthalmol*. 2007;125:908-915.
16. Yeh S, Song XJ, Farley W, Li DQ, Stern ME, Pflugfelder SC. Apoptosis of ocular surface cells in experimentally induced dry eye. *Invest Ophthalmol Vis Sci*. 2003;44:124-129.
17. Yoon KC, De Paiva CS, Qi H, et al. Expression of Th-1 chemokines and chemokine receptors on the ocular surface of C57BL/6 mice: effects of desiccating stress. *Invest Ophthalmol Vis Sci*. 2007;48:2561-2569.
18. You IC, Coursey TG, Bian F, Barbosa FL, de Paiva CS, Pflugfelder SC. Macrophage phenotype in the ocular surface of experimental murine dry eye disease. *Arch Immunol Ther Exp (Warsz)*. 2015;63:299-304.
19. Gao Y, Min K, Zhang Y, Su J, Greenwood M, Gronert K. Female-specific downregulation of tissue polymorphonuclear neutrophils drives impaired regulatory T cell and amplified effector T cell responses in autoimmune dry eye disease. *J Immunol*. 2015;195:3086-3099.
20. Stevenson W, Chen Y, Lee SM, et al. Extraorbital lacrimal gland excision: a reproducible model of severe aqueous tear-deficient dry eye disease. *Cornea*. 2014;33:1336-1341.
21. Shinomiya K, Ueta M, Kinoshita S. A new dry eye mouse model produced by exorbital and intraorbital lacrimal gland excision. *Sci Rep*. 2018;8:1483.
22. Kim CS, Jo K, Lee IS, Kim J. Topical application of apricot kernel extract improves dry eye symptoms in a unilateral exorbital lacrimal gland excision mouse. *Nutrients*. 2016;8: E750.
23. Meng ID, Barton ST, Mecum NE, Kurose M. Corneal sensitivity following lacrimal gland excision in the rat. *Invest Ophthalmol Vis Sci*. 2015;56:3347-3354.
24. Kurose M, Meng ID. Dry eye modifies the thermal and menthol responses in rat corneal primary afferent cool cells. *J Neurophysiol*. 2013;110:495-504.
25. Kaminer J, Powers AS, Horn KG, Hui C, Evinger C. Characterizing the spontaneous blink generator: an animal model. *J Neurosci*. 2011;31:11256-11267.
26. Fujihara T, Murakami T, Fujita H, Nakamura M, Nakata K. Improvement of corneal barrier function by the P2Y(2) agonist INS365 in a rat dry eye model. *Invest Ophthalmol Vis Sci*. 2001;42:96-100.
27. Higuchi A, Oonishi E, Kawakita T, Tsubota K. Evaluation of treatment for dry eye with 2-hydroxyestradiol using a dry eye rat model. *Mol Vis*. 2016;22:446-453.
28. Higuchi A, Takahashi K, Hirashima M, Kawakita T, Tsubota K. Selenoprotein P controls oxidative stress in cornea. *PLoS One*. 2010;5:e9911.
29. Bereiter DA, Rahman M, Thompson R, Stephenson P, Saito H. TRPV1 and TRPM8 channels and nocifensive behavior in a rat model for dry eye. *Invest Ophthalmol Vis Sci*. 2018;59:3739-3746.
30. Rahman M, Okamoto K, Thompson R, Katagiri A, Bereiter DA. Sensitization of trigeminal brainstem pathways in a model for tear deficient dry eye. *Pain*. 2015;156:942-950.
31. Meng ID, Kurose M. The role of corneal afferent neurons in regulating tears under normal and dry eye conditions. *Exp Eye Res*. 2013;117:79-87.
32. Suwan-Apichon O, Reyes JM, Griffin NB, Barker J, Gore P, Chuck RS. Microkeratome versus femtosecond laser pre-dissection of corneal grafts for anterior and posterior lamellar keratoplasty. *Cornea*. 2006;25:966-968.
33. Suwan-Apichon O, Rizen M, Rangsin R, et al. Botulinum toxin B-induced mouse model of keratoconjunctivitis sicca. *Invest Ophthalmol Vis Sci*. 2006;47:133-139.
34. Lee HS, Chauhan SK, Okanobo A, Nallasamy N, Dana R. Therapeutic efficacy of topical epigallocatechin gallate in murine dry eye. *Cornea*. 2011;30:1465-1472.
35. Nakamura S, Shibuya M, Nakashima H, et al. Involvement of oxidative stress on corneal epithelial alterations in a blink-suppressed dry eye. *Invest Ophthalmol Vis Sci*. 2007;48: 1552-1558.
36. Xiao X, He H, Lin Z, et al. Therapeutic effects of epidermal growth factor on benzalkonium chloride-induced dry eye in a mouse model. *Invest Ophthalmol Vis Sci*. 2012;53:191-197.
37. Chen W, Zhang X, Li J, et al. Efficacy of osmoprotectants on prevention and treatment of murine dry eye. *Invest Ophthalmol Vis Sci*. 2013;54:6287-6297.
38. Zhang Z, Yang WZ, Zhu ZZ, et al. Therapeutic effects of topical doxycycline in a benzalkonium chloride-induced mouse dry eye model. *Invest Ophthalmol Vis Sci*. 2014;55: 2963-2974.
39. de Paiva CS, Pflugfelder SC. Rationale for anti-inflammatory therapy in dry eye syndrome. *Arq Bras Oftalmol*. 2008;71: 89-95.
40. Dohlman TH, Ding J, Dana R, Chauhan SK. T Cell-derived granulocyte-macrophage colony-stimulating factor contributes to dry eye disease pathogenesis by promoting CD11b+ myeloid cell maturation and migration. *Invest Ophthalmol Vis Sci*. 2017;58:1330-1336.
41. Hamrah P, Dana MR. Corneal antigen-presenting cells. *Chem Immunol Allergy*. 2007;92:58-70.
42. Lekhanont K, Park CY, Smith JA, et al. Effects of topical anti-inflammatory agents in a botulinum toxin B-induced mouse model of keratoconjunctivitis sicca. *J Ocul Pharmacol Ther*. 2007;23:27-34.
43. Zhu L, Shen J, Zhang C, et al. Inflammatory cytokine expression on the ocular surface in the Botulium toxin B induced murine dry eye model. *Mol Vis*. 2009;15:250-258.
44. Barabino S, Chen W, Dana MR. Tear film and ocular surface tests in animal models of dry eye: uses and limitations. *Exp Eye Res*. 2004;79:613-621.
45. Lee HS, Amouzegar A, Dana R. Kinetics of corneal antigen presenting cells in experimental dry eye disease. *BMJ Open Ophthalmol*. 2017;1:e000078.
46. Ferrari G, Chauhan SK, Ueno H, et al. A novel mouse model for neurotrophic keratopathy: trigeminal nerve stereotactic electrolysis through the brain. *Invest Ophthalmol Vis Sci*. 2011;52:2532-2539.
47. Scholzen T, Gerdes J. The Ki-67 protein: from the known and the unknown. *J Cell Physiol*. 2000;182:311-322.
48. Darrt DA. Neural regulation of lacrimal gland secretory processes: relevance in dry eye diseases. *Prog Retin Eye Res*. 2009;28:155-177.

49. Barabino S, Rolando M, Chen L, Dana MR. Exposure to a dry environment induces strain-specific responses in mice. *Exp Eye Res.* 2007;84:973-977.
50. Pal-Ghosh S, Tadvalkar G, Jurjus RA, Zieske JD, Stepp MA. BALB/c and C57BL6 mouse strains vary in their ability to heal corneal epithelial debridement wounds. *Exp Eye Res.* 2008;87:478-486.
51. Yang Q, Zhang Y, Liu X, Wang N, Song Z, Wu K. A comparison of the effects of benzalkonium chloride on ocular surfaces between C57BL/6 and BALB/c mice. *Int J Mol Sci.* 2017;18:E509.
52. Watanabe H, Numata K, Ito T, Takagi K, Matsukawa A. Innate immune response in Th1- and Th2-dominant mouse strains. *Shock.* 2004;22:460-466.
53. Wang SB, Hu KM, Seamon KJ, Mani V, Chen Y, Gronert K. Estrogen negatively regulates epithelial wound healing and protective lipid mediator circuits in the cornea. *FASEB J.* 2012;26:1506-1516.
54. Krishnan T, Prajna NV, Gronert K, et al. Gender differences in re-epithelialisation time in fungal corneal ulcers. *Br J Ophthalmol.* 2012;96:137-138.
55. Suzuki T, Richards SM, Liu S, Jensen RV, Sullivan DA. Influence of sex on gene expression in human corneal epithelial cells. *Mol Vis.* 2009;15:2554-2569.
56. Sato EH, Ariga H, Sullivan DA. Impact of androgen therapy in Sjogren's syndrome: hormonal influence on lymphocyte populations and Ia expression in lacrimal glands of MRL/Mp-lpr/lpr mice. *Invest Ophthalmol Vis Sci.* 1992;33:2537-2545.
57. Sullivan DA, Edwards JA. Androgen stimulation of lacrimal gland function in mouse models of Sjogren's syndrome. *J Steroid Biochem Mol Biol.* 1997;60:237-245.
58. Yu D, Saini Y, Chen G, et al. Loss of beta epithelial sodium channel function in meibomian glands produces pseudoaldosteronism 1-like ocular disease in mice. *Am J Pathol.* 2018;188:95-110.
59. Richards SM, Yamagami H, Schirra F, Suzuki T, Jensen RV, Sullivan DA. Sex-related effect on gene expression in the mouse meibomian gland. *Curr Eye Res.* 2006;31:119-128.
60. Schirra F, Richards SM, Liu M, Suzuki T, Yamagami H, Sullivan DA. Androgen regulation of lipogenic pathways in the mouse meibomian gland. *Exp Eye Res.* 2006;83:291-296.